



# Does Biliodigestive Anastomosis Have Any Effect on the Reversal of Hepatopulmonary Syndrome in a Biliary Cirrhosis Experimental Model?

Leonardo Ervolino Corbi<sup>1</sup> · Ana Cristina Aoun Tannuri<sup>1</sup> · Maria Julia de Aro Braz<sup>1</sup> · Vitor Ribeiro Paes<sup>1</sup> · Lourenço Sbragia<sup>2</sup> · Rebeca Lopes Figueira<sup>2</sup> · Karina Miura da Costa<sup>2</sup> · Maria Cecilia Mendonça Coelho<sup>1</sup> · Josiane Oliveira Gonçalves<sup>1</sup> · Suellen Serafini<sup>1</sup> · Uenis Tannuri<sup>1</sup>

Received: 3 September 2018 / Accepted: 3 May 2019 / Published online: 10 May 2019  
© Springer Science+Business Media, LLC, part of Springer Nature 2019

## Abstract

**Background** Biliary cirrhosis is associated with hepatopulmonary syndrome (HPS), which is related to increased posttransplant morbidity and mortality.

**Aims** This study aims to analyze the pathophysiology of biliary cirrhosis and the onset of HPS.

**Methods** Twenty-one-day-old Wistar rats were subjected to common bile duct ligation and were allocated to two groups: group A (killed 2, 3, 4, 5, or 6 weeks after biliary obstruction) and group B (subjected to biliodigestive anastomosis 2, 3, 4, 5, or 6 weeks after the first procedure and killed 3 weeks later). At the killing, arterial blood was collected for the analyses, and samples from the liver and lungs were collected for histologic and molecular analyses. The gasometric parameters as well as the expression levels of ET-1, eNOS, and NOS genes in the lung tissue were evaluated.

**Results** From a total of 42 blood samples, 15 showed hypoxemia ( $pO_2 < 85$  mmHg) and 17 showed an increased oxygen gradient [ $p(A-a)O_2 > 18$  mmHg]. The liver histology revealed increased ductular proliferation after common bile duct ligation, and reconstruction of bile flow promoted decreased ductular proliferation 5 and 6 weeks post-common bile duct ligation. Pulmonary alterations consisted of decreased parenchymal airspace and increased medial wall thickness. Biliary desobstruction promoted transitory improvements 5 weeks after biliary obstruction (increased parenchymal airspace and decreased MWT— $p = 0.003$  and  $p = 0.004$ , respectively) as well as increased endothelin expression levels ( $p = 0.009$ ).

**Conclusions** The present model showed lung tissue alterations promoted by biliary obstruction. The biliodigestive anastomosis had no clear direct effects on these alterations.

**Keywords** Hepatopulmonary syndrome · Biliary cirrhosis · Experimental animal model · Bile duct obstruction · Biliary desobstruction · Cirrhosis reversibility

## Introduction

During the evolution of cirrhosis and liver failure in children, hepatopulmonary syndrome (HPS) is an important consequence of liver disease. This syndrome is defined by the presence of liver disease or portal hypertension and pulmonary intravascular dilation, causing an abnormal alveolar–arterial oxygen gradient [1]. The syndrome is present in 5–32% of cirrhotic patients [2] and in up to 20% of children

with biliary atresia [3]. The onset of HPS indicates poor prognosis and higher mortality in these groups of patients with cirrhosis, mainly in the postoperative period of liver transplantation.

The pathophysiology of HPS is not completely known, although several conclusions have been taken from experimental models of common bile duct ligation. These models showed that the syndrome is due to increased endothelial nitric oxide synthase (eNOS) expression, with a higher production of nitric oxide (NO) and consequent vasodilation. This increased eNOS expression is due to the production of endothelin-1 (ET-1) by cholangiocytes of the cirrhotic liver and activation of endothelial endothelin B (ETB) receptors in the pulmonary vascular endothelium, producing a

✉ Uenis Tannuri  
uenist@usp.br

Extended author information available on the last page of the article

vasodilatory effect. Studies of these experimental models also observed the intravascular accumulation of macrophages expressing nitric oxide synthase (NOS) and heme-oxygenase-1, resulting in a higher production of NO and CO, respectively, contributing to the vasodilatory effects [4]. In humans, a correlation between ET-1 levels in hepatic venous blood and intrapulmonary vasodilation in patients with cirrhosis has been observed, both of which are associated with ductular proliferation in the liver of these patients [5].

Angiogenesis has also been observed in experimental models of HPS derived from the release of vascular endothelial growth factor (VEGF-A) by accumulating macrophages in the pulmonary vasculature. It is not known exactly which factor triggers this accumulation, although some studies suggest a role for tumor necrosis factor (TNF), related to the translocation of bacterial endotoxins, ET-1, and possibly monocyte-directed chemokines [2].

There is no effective treatment for HPS other than a liver transplant, which is followed by remission of the disease in more than 80% of cases, especially in children [1]. However, some drugs, such as pentoxifylline, somatostatin, L-nitroarginine methyl ester (L-NAME), and aspirin, have been tested in patients with no clear positive effects [2].

Despite advances in research on HPS, several aspects of its pathophysiology remain unclear. In addition, studies are based on experimental models in adult animals, which are of lesser value for pediatric clinical situations. The present study had the objective of better understanding the pathophysiology of HPS in child candidates for liver transplantation, based on an experimental model with young animals subjected to common bile duct ligation. The specific objectives were as follows:

- To determine how long after the common bile duct ligation the HPS starts, correlating the time with the degree of liver cirrhosis;
- To verify whether the syndrome can be reversed after reconstruction of the bile flow and how long after bile duct ligation this procedure is effective;
- To study lung histologic modifications in this animal model.

## Materials and Methods

One hundred and twenty-nine 21-day-old Wistar rats of both sex underwent biliary obstruction, which was performed after anesthesia with doses of 30 mg/kg of ketamine hydrochloride (Ketalar<sup>®</sup>) and 10 mg/kg of dexmedetomidine (Precedex<sup>®</sup>).

The animals were cared for according to the criteria outlined in the “Guide for Care and Use of Laboratory Animals” prepared by the National Academy of Sciences. The

study protocol was reviewed and approved by the Animal Ethics Committee at our institution (University of São Paulo Medical School, São Paulo, Brazil).

The rats that underwent only common bile duct ligation (group A) were divided into the subgroups A1, A2, A3, A4, and A5 and were killed 2, 3, 4, 5, and 6 weeks, respectively, after the bile duct ligation. The animals in group B were subdivided into the subgroups B1, B2, B3, B4, and B5 and were subjected to biliary reconstruction 2, 3, 4, 5, and 6 weeks, respectively, after the bile duct ligation. All the animals of this group were killed 3 weeks after the second operation.

## Operations

The common bile duct ligation was performed under anesthesia with 30 mg/kg of ketamine hydrochloride (Ketalar<sup>®</sup>) and 10 mg/kg of dexmedetomidine (Precedex<sup>®</sup>). The procedure consisted of performing a 3-centimeter median longitudinal incision under the xiphoid process, with visualization of the liver and intestines. The common bile duct was visualized and ligated with nylon 6-0. Then, the abdominal contents were returned to the abdominal cavity, and the wall was closed in a single layer with nylon 4-0.

The biliary reconstruction consisted of performing an anastomosis between a jejunal loop and the cyst formed on the proximal portion of the ligated bile duct. The anastomoses were performed with Prolene 7-0, and the abdominal cavity was closed in the same fashion as in the bile duct ligation surgery.

At the time of killing, the animals were anesthetized and subjected to wide longitudinal laparotomy for visualizing the abdominal aorta, and arterial blood was collected for gasometry.

The trachea was surgically exposed and cannulated with a 22G catheter. Then, the liver and lung samples were collected for molecular, histologic, and histomorphometric analyses. The lungs were inflated and fixed at 23 cm pressure with 4% paraformaldehyde in phosphate-buffered solution. All the study groups are schematically shown in Fig. 1.

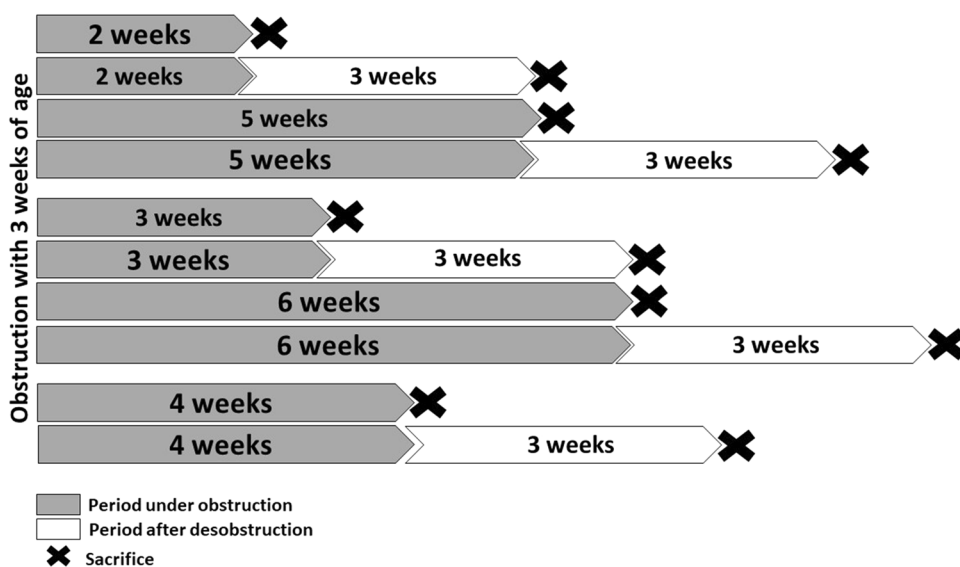
## Biochemical Analyses

The partial pressure values of O<sub>2</sub> and CO<sub>2</sub> were used for the calculation of the arterial–alveolar gradient of O<sub>2</sub>, utilizing the formula  $150 - (PaCO_2/0.8) - PaO_2$  [6]. HPS was defined as  $PaO_2 < 85$  mmHg and  $P(A-a)O_2 > 18$  mmHg [7].

## Histology and Histomorphometry

The hepatic and pulmonary tissues were fixed in formalin and embedded in paraffin. The hepatic tissue sections were stained with hematoxylin–eosin (HE) and blindly analyzed by two pathologists under an optical microscope for general

**Fig. 1** Schematic demonstration of the study groups. The rats with 3 weeks of age underwent biliary obstruction, and the biliary reconstruction was performed after 2, 3, 4, 5, and 6 weeks, as indicated



observation of the parenchymal morphology and ductular proliferation. For ductular proliferation counting, five randomly chosen fields per slide containing at least one portal space were analyzed. The measurements in each field were made semiquantitatively using a score ranging from zero to 3, wherein zero corresponded to the absence of findings; 1 corresponded to a slight alteration; 2 corresponded to a moderate alteration; and 3 corresponded to an intense alteration.

The pulmonary tissue was observed as to the histologic alterations responsible for the pulmonary shunt, i.e., the parenchymal airspace and vascular measurements. The stained lung sections were photographed using a light microscope (NIKON Eclipse E200 80i, Tokyo, Japan) at 20× magnification, and the images were analyzed using Image J (National Institutes of Health, Bethesda, MD, USA). First, the scaling of the images was globally set using the Analyze/Set Scale command. To measure the total lung parenchymal area, the images were subjected to the color threshold function using Image–Adjust–Color Threshold–Analyze–Measure, and then the air space was measured by the subtraction of the parenchymal area from the total area. We measured ten fields per animal and four animals per group [8]. The results are expressed in pixels/μm, and  $p < 0.05$  was considered significant. The preacinar resistance arterioles between 30 and 60 μm were photographed using a light microscope at 40× magnification, and the images were analyzed using Image J. We measured the external diameter (ED) and internal diameter (ID) and calculated the proportional medial wall thickness (MWT) with the following formula:  $MWT = (ED - ID) / ED$ . This proportion eliminates the effects of vasodilation, constriction, and sample fixation over the morphometric variables [9]. The parameters were measured from ten different vessels per animal in four animals per group.

## Molecular Biology

Gene expression alterations in the lung tissue were detected by real-time RT-PCR methodology. The expression levels of ET-1, NOS, and eNOS genes were evaluated.

Total RNA was isolated from frozen tissue samples using TRIZOL (Invitrogen, USA) according to the manufacturer's protocol. Total RNA was quantified with spectrophotometry using a BioPhotometer (Eppendorf AG, Germany) at an absorbance of 260 nm, and the purity was assessed using the 260/280 nm absorbance ratio. This value ranged from 1.8 to 2.0 for all samples. The integrity of the isolated RNA samples was determined by agarose gel electrophoresis and ethidium bromide staining of the 18S and 28S ribosomal RNA bands.

Complementary DNA (cDNA) was prepared from 2 μg total RNA by reverse transcription using 200 U of SuperScript III RNase H-RT (Invitrogen) and oligo (dT) primers. The resulting cDNA was stored at  $-20^{\circ}\text{C}$ .

Primers specific for the genes were designed based on the rat messenger RNA sequences from the GenBank database using the Primer 3 software (<http://www.bioinformatics.nl/cgi-bin/primer3plus/primer3plus.cgi/>). As an internal reference, primers for hypoxanthine phosphoribosyltransferase were used. The primer sequences and size of the amplified products are listed in Table 1.

qRT-PCR was performed using the Rotor-Gene Q 5plex HRM thermal cycler (Qiagen, Germany). Each 15 μL reaction contained 100 ng cDNA, 0.3 μL gene-specific forward and reverse primers (10 μM), and 7.5 μL Platinum Sybr Green qRT-PCR SuperMix-UDG kit (Invitrogen). The cycling conditions were as follows: initial template denaturation for 5 min at  $95^{\circ}\text{C}$ , followed by 40 cycles of denaturation

**Table 1** List of primer sequences and size of products

Gene	Forward primer 5'–3'	Reverse primer 5'–3'	Size (bp)
Endothelin-1	GTT CCA AAC ATT CCA AGA GAG G	CTG AGT CAG ACA CGA ACA CTC C	232
eNOS	GTG ACC CTC ACC GAT ACA A	CTG GCC TTC TGC TCA TTT TCC	210
NOS	TTC AGA AGC AGA ATG TGA CCA	GTT CAA TAT CTC CTG GTG GAA C	169
HPRT	CTC ATG GAC TGA TTA TGG ACA GGA C		123

*bp* base pair

at 95 °C for 20 s, and annealing at 60 °C for 30 s. Fluorescence detection was performed during each cycle at 72 °C to identify the positive samples. Each sample was assessed in triplicate, and controls without template were included in parallel for each reaction. Amplification was followed by a melting curve analysis to check PCR product specificity. The fold changes in gene expression relative to the levels obtained in healthy rats, which were set equal to 1, were analyzed and calculated using the  $2^{-\Delta\Delta ct}$  method.

## Statistics

The animals subjected to the obstruction and reconstruction of biliary flow were compared with their respective time periods in the group subjected only to biliary obstruction. The changes observed in different time periods in the same group were also evaluated. The intragroup comparisons (different periods after the surgical procedures) and intergroup comparisons (same period after the surgical procedures) were made by using the ANOVA test. Finally, we made additional comparisons between groups A and B, at the same time points after the biliary obstruction—5 and 6 weeks. For nonparametric data comparisons, the Kruskal–Wallis test was used. The hypothesis of equality was rejected for  $p \leq 0.05$ .

## Results

### Mortality

The mortality rate of the groups was 39.8% after the first surgery and 56.7% after the second surgery. At the end of the experiment, each subgroup had a minimum of five surviving animals.

### Biochemical Analyses: Gasometric Studies

From a total of 65 animals with blood samples collected, we obtained 15 animals with the criteria for hypoxemia and 17 with an elevated alveolar–arterial oxygen gradient. Regarding the pO<sub>2</sub>, we found no difference when comparing groups A1 to A5 ( $p=0.207$ ) or when comparing between groups

A and B ( $p=0.741$ ). We observed an increase in the arterial–alveolar gradient of O<sub>2</sub> as time passed after obstruction in group A (with the exception of group A1), but this result was not reproduced in group B. There were significant differences among groups A1 through A5 (A2 vs. A5  $p=0.011$ ; A3 vs. A5  $p=0.016$ ; Fig. 2).

### Histology and Histomorphometry

**Liver** The analysis of liver histology revealed aspects of biliary cirrhosis and increased ductular proliferation with time after the common bile duct ligation (Fig. 3). The animals that underwent reconstruction of bile flow showed less ductular proliferation. There were differences among groups A1 through A5 ( $p=0.007$ ) and between groups A and B ( $p=0.019$  and  $p=0.001$  at 5 and 6 weeks post-common bile duct ligation, respectively), although no differences were noted among groups B1 through B5 ( $p=0.246$ ; Fig. 4a, d).

**Lung** We observed the presence of inflammatory cells and thickened septa, as well as areas with normal lung tissue (Fig. 5). It was verified that desobstruction promoted transitory improvements 5 weeks after biliary obstruction (increased parenchymal airspace and decreased MWT;  $p=0.003$  and  $p=0.004$ , respectively). These changes were reversed in the sixth week after obstruction (Fig. 4b–f).

### Molecular Biology Studies

**Endothelin** We observed a decrease in the expression of endothelin with time after biliary obstruction in both groups A and B ( $p=0.04$  and  $p=0.011$ , respectively). It was verified that desobstruction promoted increased endothelin expression levels 5 weeks after the biliary obstruction procedure ( $p=0.009$ ; Fig. 6d).

**eNOS** The intragroup comparisons did not show any differences regarding eNOS expression levels, although a decrease was noted when desobstructed animals after 5 and 6 weeks were compared with obstructed animals ( $p=0.008$ ,  $p=0.03$ ; Fig. 6b). However, the comparisons at the same time after the biliary obstruction did not show differences (Fig. 6e).

**NOS** There were no significant differences in NOS expression among groups A1 through A5 ( $p=0.167$ ) or

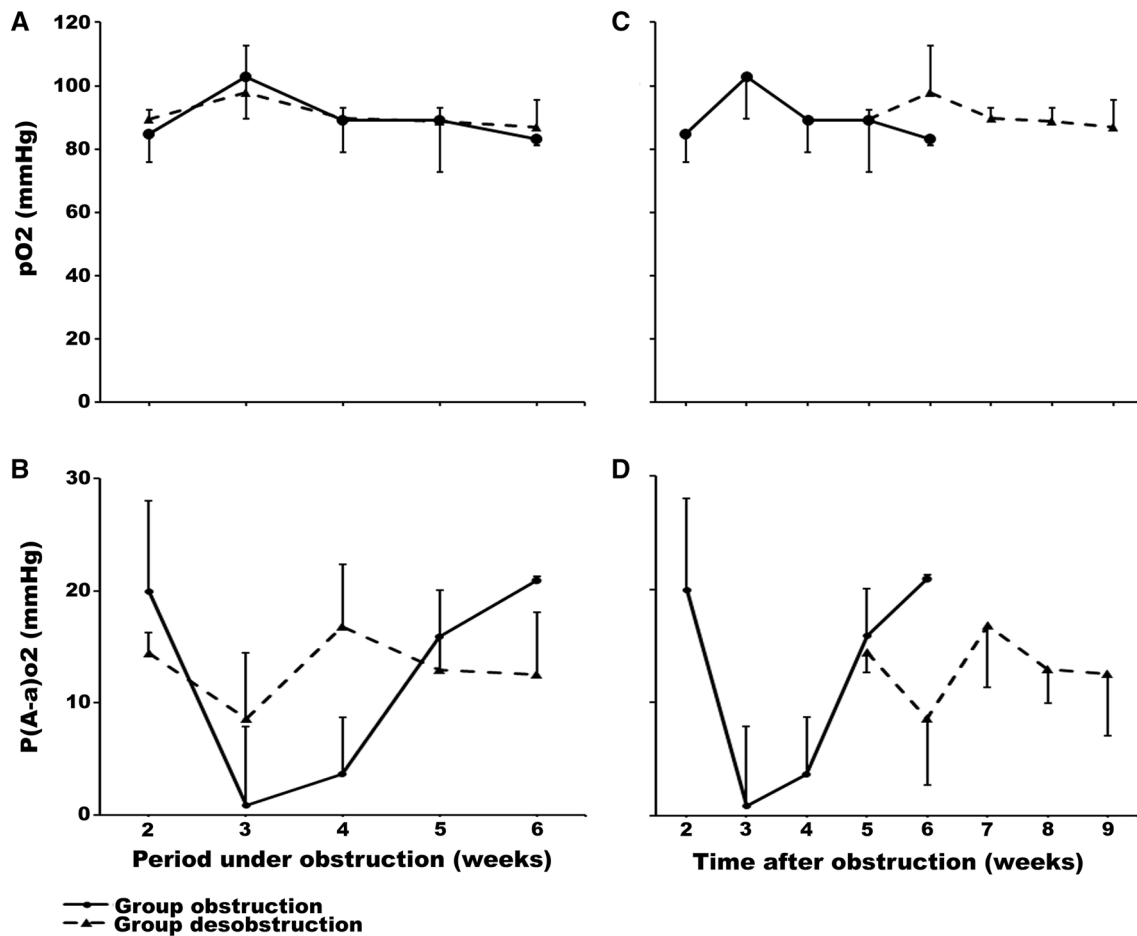


**Fig. 2** Results of the gasometric studies (mean  $\pm$  standard error of the mean). **a** Note the differences in the arterial–alveolar gradient of O<sub>2</sub>: A2 vs. A5  $p=0.011$ ; A3 vs. A5  $p=0.016$ . **b** No differences were observed. ( $N$  per group varied from 5 to 7.) No differences were observed in pO<sub>2</sub> values when comparing subgroups A1 to A5 ( $p=0.207$ ) or groups A and B ( $p=0.741$ ). Note that it was verified

an increase in the arterial–alveolar gradient of O<sub>2</sub> as time passed after obstruction in group A (with the exception of subgroup A1), but this result was not observed in group B. Finally, significant differences among subgroups A1 through A5 were observed (A2 vs. A5  $p=0.011$ ; A3 vs. A5  $p=0.016$ ). The number of animals in each subgroup varied from 5 to 7

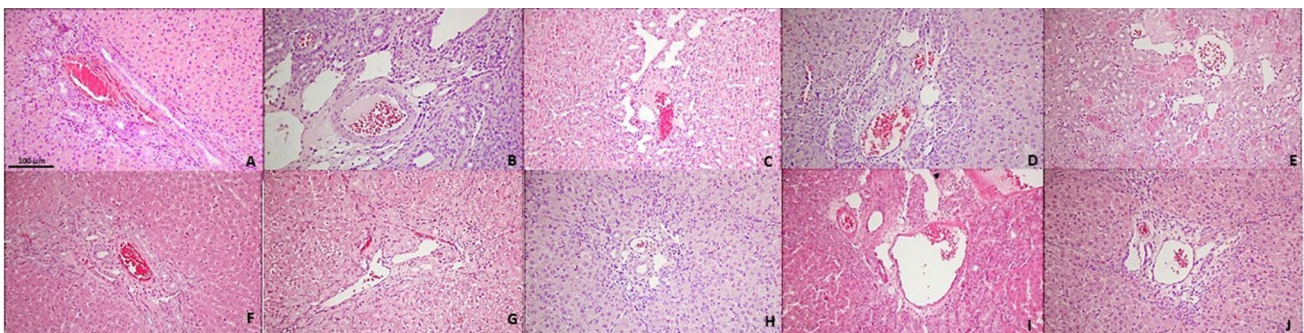


**Fig. 3** Histology of liver of the study groups. Note the ductular proliferation in portal space in all subgroups (**a, b, c, d, e**, common bile duct ligation after 2, 3, 4, 5, and 6 weeks, respectively; **f, g, h, i, j**,

biliary reconstruction performed 2, 3, 4, 5, and 6 weeks after the bile duct ligation, respectively. HE magnification 200 $\times$ )

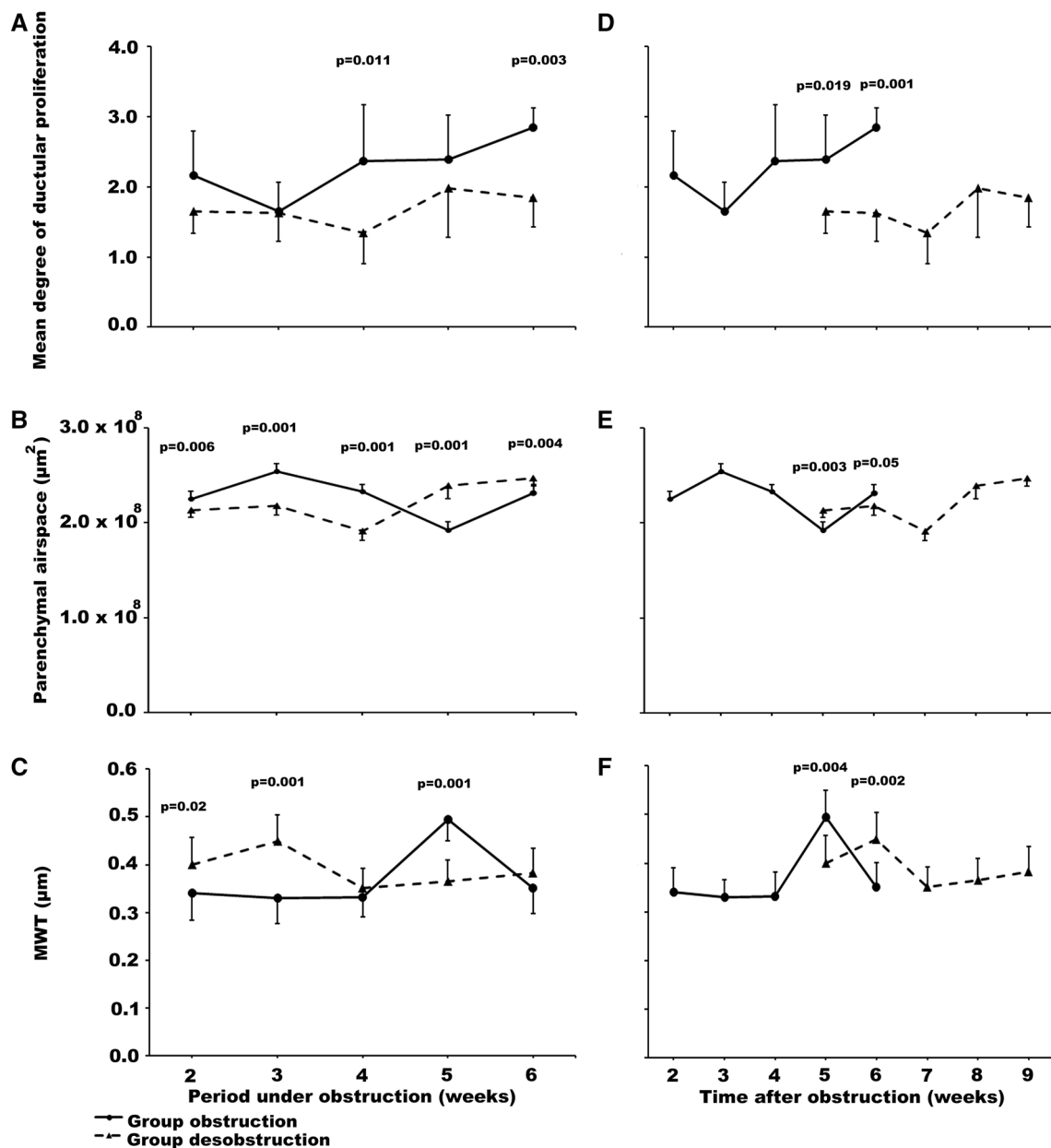


**Fig. 4** Results of the liver and lung histomorphometric studies (mean  $\pm$  standard error of the mean). **a** and **d**—liver histomorphometry—note that the animals that underwent reconstruction of bile flow showed less ductular proliferation. There were differences among subgroups A1 through A5 ( $p=0.007$ ) and between groups A and B ( $p=0.019$  and  $p=0.001$  at 5 and 6 weeks post-common bile duct ligation, respectively), although no differences were noted among

subgroups B1 through B5 ( $p=0.246$ ; Fig. **a** and **d**). Figure **b**, **c**, **e**, **f**—lung histomorphometry: Note that desobstruction promoted transitory improvements 5 weeks after biliary obstruction (increased parenchymal airspace and decreased MWT;  $p=0.003$  and  $p=0.004$ , respectively). These changes were reversed in the sixth week after obstruction (**b**, **e**, **c**, and **f**). *N* per subgroup varied from 5 to 7

between groups A and B ( $p=0.182$ ) (Fig. **6c**). The comparisons of desobstructed animals after 5 and 6 weeks with obstructed ones did not show any difference (Fig. **6d**).

### Discussion

The current knowledge of HPS remains incomplete and is based on animal models. Although its natural history is not defined, the only well-established, efficient treatment for this condition is liver transplantation, even in cases when liver function is not critically insufficient. The known

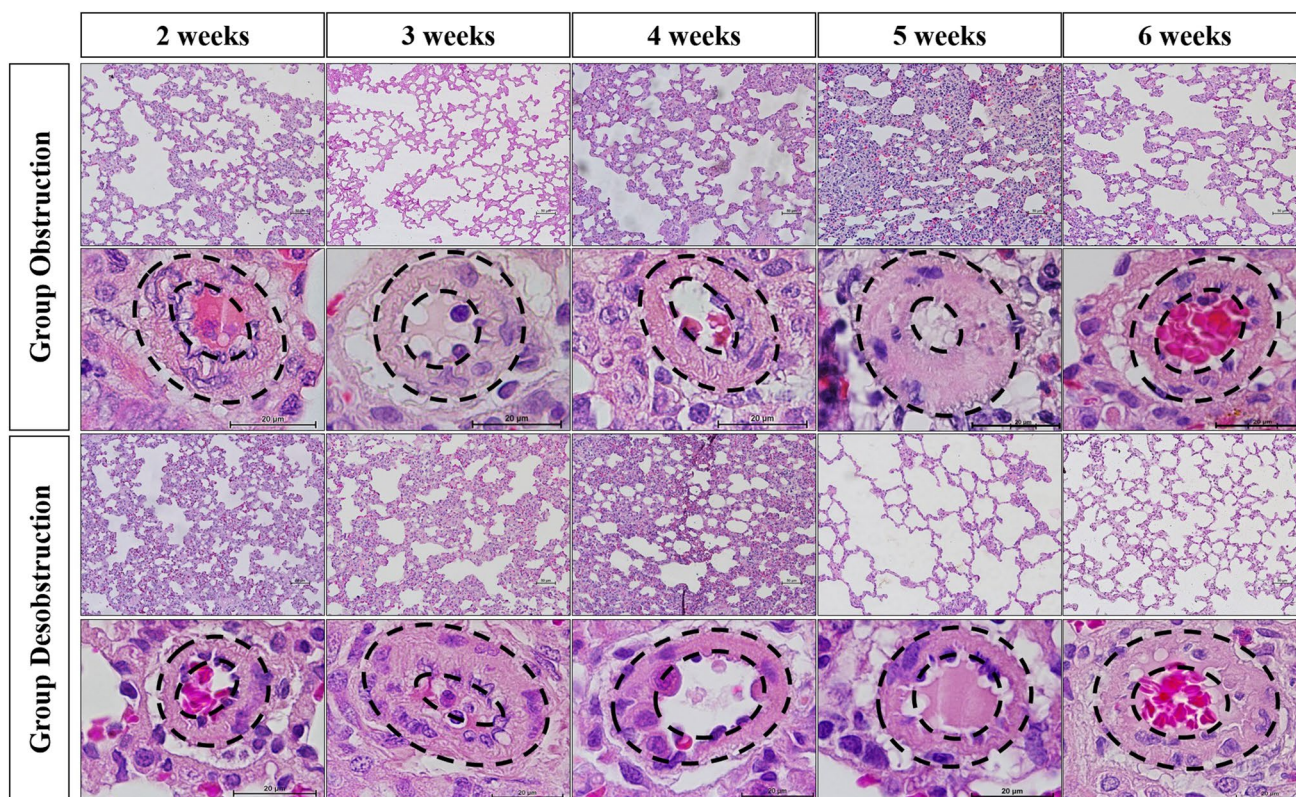


**Fig. 5** Histologic aspects of lungs in the groups of study. Note the increased parenchymal airspace in the desobstructed animals after 5 weeks (HE parenchyma figures: magnification 200 $\times$ ; arteriole figures: magnification 1000 $\times$ )

pathophysiology of the syndrome consists of unbalanced gas exchange at the pulmonary level due to greater expression of NOS, especially pulmonary eNOS, secondary to the production of endothelin by hepatic cholangiocytes [1, 10, 11].

The first criticism to the current study is based on the high mortality rates of the animals. In fact, these rates are due to the young age, small size, friability of tissues of weaning rats, and susceptibility to anesthetic drugs. However, we noticed that mortality increased as time passed after biliary ligation and, consequently, as cirrhosis worsened. So, few animals died during the first week after biliary ligation (around 15% of operated rats), and these deaths were related to anesthetic or operative complications. During the second and third postoperative weeks, mortality index decreased (around 5–10%), and the causes were probably linked to the metabolic alterations provoked by liver cirrhosis. From the fourth week on, we observed that animals became icteric and lethargic, and the final mortality indexes increased between the fourth and sixth weeks (close to 40%). During the second procedure, we noted the presence of many abdominal adhesions that had to be sectioned to access the biliary cyst and perform the bilioenteric anastomosis. As the animals were cirrhotic, bleeding due to the sectioning of these adhesions was

more intense and the mortality was higher. About 20% of rats of subgroups B1 and B2 died, mainly during the first postoperative days. In subgroups B3, B4, and B5, mortality indexes were progressively higher, and the deaths occurred mainly during the first days, as their health status was severely impaired by liver cirrhosis.

Another hypothetical bias of the current study is that only the animals that did not die spontaneously were evaluated. However, even in surviving animals, we observed that cirrhosis worsened as time after biliary ligation passed, and bilioenteric anastomosis was able at least to partially reverse it, as previously described [12]. We believe that most of the deaths occurred due to operative-related complications and liver cirrhosis, and not due to hepatopulmonary syndrome itself. The animals that naturally died were apathetic and hypoactive, but none of them presented with cyanosis or tachydyspnea, what made us believe that no selection bias related to the severity of hepatopulmonary syndrome occurred, so the results and conclusions of the present study are valid. Finally, regarding the gender of animals in this study, we opted for utilizing animals of both sex, as the main cholestatic diseases of childhood affect females and males (with a slightly higher prevalence in girls), without any difference related to severity between

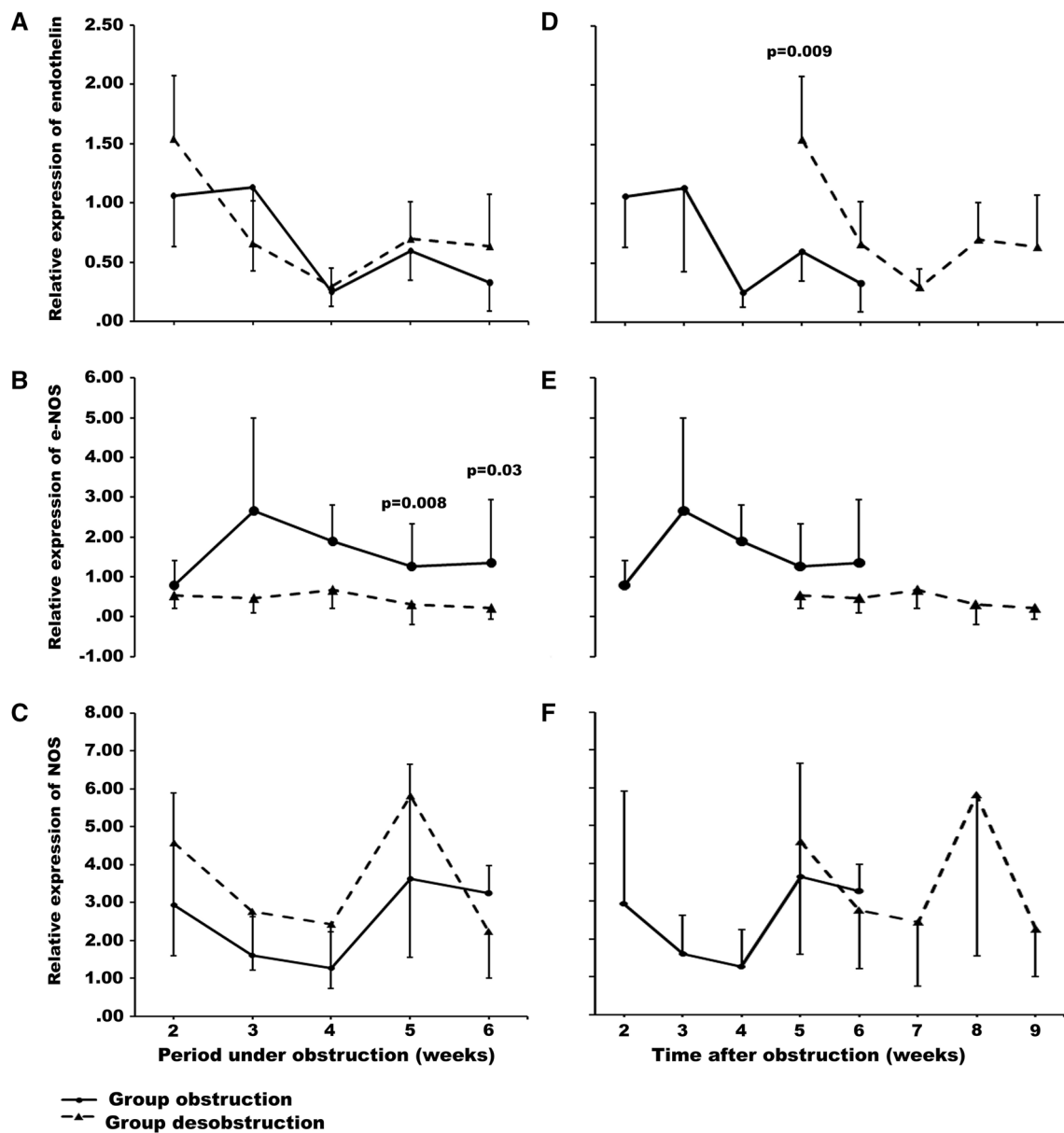


**Fig. 6** Results of molecular biology studies. **b** Regarding eNOS levels, the values of *p* refer to the comparisons between obstructed and desobstructed animals after 5 and 6 weeks. **d**—the value of *p* refers

to the comparison between obstructed and desobstructed animals, at 5 weeks after the biliary obstruction. (*N* per subgroup varied from 5 to 7)

genders. In our study, similarly, no differences between female and male rats about mortality or gene expression levels could be detected.

Some previous experimental investigations on HPS and biliary cirrhosis have been published, although none were performed in 3-week-old weaning animals. Shikata et al. [13] obtained significantly lower values of  $pO_2$  and  $p(A-a)O_2$  in an 8-week-old mouse biliary ligation model. In addition, they found alterations in pulmonary morphology with HE, with progressive worsening with time after biliary ligation. Furthermore, Yang et al. [14] observed a reduction in

total lung volume and alveolar space in adult rats subjected to biliary ligation in comparison with the control animals.

In the current study, we searched for a relationship between the expression of vascular mediators and the development of biliary cirrhosis and HPS in a young rat model of cirrhosis provoked by common bile duct ligation. We previously described this model and we added the biliary cyst-jejunal anastomosis in order to study the reversibility of biliary cirrhosis [12]. It was proved that the histologic and molecular changes in the liver parenchyma promoted by biliary obstruction can be partially reversed by a biliary



drainage procedure. Now, we aimed to study the effects of the biliary desobstruction over the pulmonary changes provoked by the biliary cirrhosis. For this purpose, we had to make comparisons between biliary obstructed and desobstructed animals, although there was a delay of time between these groups. Despite this objection, we consider that these comparisons were valid since the desobstruction surgery was the most important difference between the groups.

In fact, we observed an increase in ductular proliferation with the advance of time after biliary ligation, as well as a partial resolution of the process characterized by lower proliferation in the animals subjected to bile flow reconstruction. These differences were confirmed when the comparisons were made between obstructed and desobstructed animals at the same points after the biliary obstruction procedure (Fig. 4d). Therefore, we were able to reproduce liver disease (and reversion) in order to study lung disease and this is an important original contribution of the current investigation.

As for the pulmonary manifestations, hypoxia was produced in 15 animals and an altered alveolar–arterial  $O_2$  gradient was produced in 17 animals, consistent with the observation in clinical practice of incidence of HPS in only some patients with cirrhosis [1]. Even with a large number of samples, the number of animals with gasometric changes remained small and inconstant, with no apparent association with time of biliary obstruction (and despite the desobstruction procedure), the degree of ductular proliferation, or the expression of endothelin, NOS, or eNOS. This result may be due to the heterogeneity of the presentation and installation of HPS, making it difficult to identify the triggers and relationships between liver injury, systemic inflammatory response mediators and gasometric manifestations.

The pulmonary tissue, in turn, showed several changes even without clear correlations with the gasometric and molecular patterns. We observed the presence of inflammation, thickening and vascular engorgement of the alveolar septa, with apparent progression according to the time of biliary obstruction and hepatic injury in group A.

In group B, however, the reestablishment of biliary flow did not promote a clear impact in the progression of lung damage. Similarly, the alveolar–arterial oxygen gradient in desobstructed animals seemed to be stable as time elapsed after surgery. These findings suggest that hepatic stimuli that cause the development of vascular and parenchymal lung alterations cannot be reversed by the biliodigestive anastomosis.

Interestingly, endothelin expression in the lung tissue decreased with time after biliary obstruction, in both groups of study. In addition, the comparisons of results obtained 5 weeks after the biliary obstruction showed increased expression levels promoted by the biliodigestive anastomosis ( $p=0.009$ ). It was previously shown that ET-1 levels

increased nearly threefold 1 week after common bile duct ligation and did not correlate with the progression of liver injury or the degree of portal hypertension, in contrast to human cirrhosis. Hepatic and plasma endothelin-1 reportedly increased after bile duct ligation and are accompanied by increased hepatic endothelin-1 mRNA and increased endothelin-1 protein in the biliary epithelium [11]. However, the elevation of pulmonary ET-1 expression is not consistent among different studies, and it seems that increased circulating levels of ET-1 lead to increased lung vascular ETB receptor expression [15]. Therefore, the onset of HPS is hypothesized to be triggered by the ET-1/ETB receptor activation of eNOS-derived NO production in the pulmonary endothelium. In fact, an attenuation in experimental HPS was observed in endothelin B receptor-deficient adult rats after CBDL [1]. Most likely, similar pathways occur in weaning cholestatic rats, and the decrease in ET-1 lung expression is a negative feedback response deflagrated by the increase in endothelin receptor expression stimulated by plasma ET-1. Finally, we may conclude that the initial cholestatic stimulus is the most important phenomenon in these alterations, as the evolution of lung ET-1 expression in obstructed and desobstructed animals seemed to be similar as shown in Fig. 6a.

As mentioned before, the upregulation of eNOS with the subsequent increased production of NO and pulmonary vasodilation plays a central role in HPS development. In our animals, the expression of eNOS in the lung tissue was not influenced by the biliodigestive anastomosis. Liu et al. studied the effect of biliary cyst fluid from common bile duct-ligated rats in the expression of endothelial nitric oxide synthase in bovine pulmonary artery endothelial cells. In fact, they observed that biliary cyst fluid increased eNOS expression and activity in an ETB receptor-dependent manner in this cell culture environment, hypothesizing that biliary obstruction results in the release of mediators such as ET-1 from the obstructed biliary tree, and these mediators reached the systemic circulation and pulmonary vasculature via disruption of the canalicular paracellular barrier [16]. In the current study, we observed a decrease in the eNOS expression levels when desobstructed animals after 5 and 6 weeks were compared with obstructed animals ( $p=0.008$ ,  $p=0.03$ ) and this finding could be explained by a positive effect of the biliodigestive anastomosis, although the comparisons at the same time after the biliary obstruction did not show differences.

Nitric oxide (NO) is related to intrapulmonary vascular dilation and the impairment of arterial oxygenation in HPS. Animal models and patients with HPS present with excessive release of NO in the lungs from the vascular endothelium due to the overexpression of eNOS [1, 2] and/or the expression of inducible NOS (iNOS) [3, 4] or from macrophages [4, 5]. Mizumoto et al. evaluated the expression

of iNOS and constitutive NOS (cNOS) in the liver, spleen, lung, and aorta in CCl<sub>4</sub>-induced cirrhotic adult rats. An increase in iNOS mRNA was found in all organs from the cirrhotic rats, especially in the lungs. No alterations in cNOS mRNA levels were found in any of the studied organs [17]. In our study, the total NOS lung expression was similar between groups A and B and among different time periods after biliary obstruction. It is possible that the age of our animals and the different methods of inducing cirrhosis are related to the discrepancies between our results and those from Mizumoto's investigation.

Finally, a criticism of our study is based on the short period of observation after the reversal of biliary obstruction. In fact, in children with HPS submitted to liver transplantation, it was shown that reversal of intrapulmonary shunting is time dependent and a long-term follow-up should be considered for accurate assessment of beneficial results after liver transplantation [18].

In conclusion, biliary obstruction in weaning rats was responsible for gasometric, histologic, and molecular pulmonary alterations, making this a useful model to better understand infantile HPS. The procedure of biliary drainage was responsible for a partial regression, or at least a stop in the progression, of some of these alterations, suggesting that the reversal of cholestasis or liver fibrogenic stimuli may be beneficial for children with cirrhosis with HPS. However, further studies are needed to clarify the mechanisms that lead some children with cirrhosis to develop HPS and to determine the adequate approaches to avoid or treat this condition.

**Author's contribution** LEC, ACAT, MJAB, and VRP performed the animal experiments; LS, RLF, KMC, MCMC, JOG, and SS performed all laboratory procedures; and UT revised the manuscript.

## Compliance with Ethical Standards

**Conflict of interest** The authors declare that they have no conflict of interest.

**Ethical approval** All applicable international, national, and institutional guidelines for the care and use of animals were followed.

## References

- Zhang J, Fallon MB. Hepatopulmonary syndrome: update on pathogenesis and clinical features. *Nat Rev Gastroenterol Hepatol*. 2012;9:539–549.
- Barbe T, Losay J, Grimon G, et al. Pulmonary arteriovenous shunting in children with liver disease. *J Pediatr*. 1995;126:571–579.
- Rodríguez-Roisin R, Krowka MJ, Hervé P, Fallon MB. ERS task force pulmonary-hepatic vascular disorders (PHD) scientific

- committee. Pulmonary–hepatic vascular disorders (PHD). *Eur Respir J*. 2004;24:861–880.
- Koch DG, Fallon MB. Hepatopulmonary syndrome. *Curr Opin Gastroenterol*. 2014;30:260–264.
- Koch DG, Bogatkevich G, Ramshesh V, et al. Elevated levels of endothelin-1 in hepatic venous blood are associated with intrapulmonary vasodilatation in humans. *Dig Dis Sci*. 2012;57:516–523. <https://doi.org/10.1007/s10620-011-1905-6>.
- Chang CC, Chuang CL, Lee FY, et al. Sorafenib treatment improves hepatopulmonary syndrome in rats with biliary cirrhosis. *Clin Sci (Lond)*. 2013;124:457–466.
- Chen L, Li YS, Cui J, et al. MiR-206 controls the phenotypic modulation of pulmonary arterial smooth muscle cells induced by serum from rats with hepatopulmonary syndrome by regulating the target gene, annexin A2. *Cell Physiol Biochem*. 2014;34:1768–1779.
- Xiao R, Goldklang MP, D'Armiento JM. Parenchymal airspace profiling: sensitive quantification and characterization of lung structure evaluating parenchymal destruction. *Am J Respir Cell Mol Biol*. 2016;55:708–715.
- Shehata SM, Mooi WJ, Okazaki T, El-Banna I, Sharma HS, Tibboel D. Enhanced expression of vascular endothelial growth factor in lungs of newborn infants with congenital diaphragmatic hernia and pulmonary hypertension. *Thorax*. 1999;54:427–431.
- Lv Y, Fan D. Hepatopulmonary syndrome. *Dig Dis Sci*. 2015;60:1914–1923. <https://doi.org/10.1007/s10620-015-3593-0>.
- Ling Y, Zhang J, Luo B, et al. The role of endothelin-1 and the endothelin B receptor in the pathogenesis of hepatopulmonary syndrome in the rat. *Hepatology*. 2004;39:1593–1602.
- de Aro Braz MJ, Corbi LE, Tannuri ACA, et al. Analysis of the reversibility of biliary cirrhosis in young rats submitted to biliary obstruction. *J Pediatr Surg*. 2018;53:1408–1413.
- Shikata F, Sakae T, Nakashiro K, et al. Pathophysiology of lung injury induced by common bile duct ligation in mice. *PLoS ONE*. 2014;14:e94550.
- Yang W, Hu B, Wu W, et al. Alveolar type II epithelial cell dysfunction in rat experimental hepatopulmonary syndrome (HPS). *PLoS One*. 2014;24:e113451.
- Gómez F, Barberà JA, Roca J, Burgos F, Gistau C, Rodríguez-Roisin R. Effects of nebulized N(G) nitro L-arginine methyl ester in patients with hepatopulmonary syndrome. *Hepatology*. 2006;43:1084–1091.
- Liu L, Zhang M, Luo B, Abrams GA, Fallon MB. Biliary cyst fluid from common bile duct-ligated rats stimulates endothelial nitric oxide synthase in pulmonary artery endothelial cells: a potential role in hepatopulmonary syndrome. *Hepatology*. 2001;33:722–727.
- Mizumoto M, Arai S, Furutani M, et al. NO as an indicator of portal hemodynamics and the role of iNOS in increased NO production in CCl<sub>4</sub>-induced liver cirrhosis. *J Surg Res*. 1997;70:124–133.
- Jin X, Sun BJ, Song JK, et al. Time-dependent reversal of significant intrapulmonary shunt after liver transplantation. *Korean J Intern Med*. 2018; Mar 5. <https://doi.org/10.3904/kjim.2017.152>. [Epub ahead of print].

**Publisher's Note** Springer Nature remains neutral with regard to jurisdictional claims in published maps and institutional affiliations.

## Affiliations

Leonardo Ervolino Corbi<sup>1</sup> · Ana Cristina Aoun Tannuri<sup>1</sup> · Maria Julia de Aro Braz<sup>1</sup> · Vitor Ribeiro Paes<sup>1</sup> · Lourenço Sbragia<sup>2</sup> · Rebeca Lopes Figueira<sup>2</sup> · Karina Miura da Costa<sup>2</sup> · Maria Cecilia Mendonça Coelho<sup>1</sup> · Josiane Oliveira Gonçalves<sup>1</sup> · Suellen Serafini<sup>1</sup> · Uenis Tannuri<sup>1</sup>

Leonardo Ervolino Corbi  
leonardo.corbi@hotmail.com

Ana Cristina Aoun Tannuri  
cristannuri@hotmail.com

Maria Julia de Aro Braz  
maria.julia.braz@usp.br

Vitor Ribeiro Paes  
vrpaes@gmail.com

Lourenço Sbragia  
sbragia@fmrp.usp.br

Rebeca Lopes Figueira  
rebecafigueira@usp.br

Karina Miura da Costa  
kari\_miura@yahoo.com.br

Maria Cecilia Mendonça Coelho  
maria.cecilia@fm.usp.br

Josiane Oliveira Gonçalves  
josi\_ogoncalves@hotmail.com

Suellen Serafini  
suellen.s@hc.fm.usp.br

<sup>1</sup> Pediatric Surgery Division, Pediatric Liver Transplantation Unit and Laboratory of Research in Pediatric Surgery (LIM 30), University of Sao Paulo Medical School, São Paulo, Brazil

<sup>2</sup> Laboratory of Experimental Fetal and Neonatal Surgery, Division of Pediatric Surgery - Department of Surgery and Anatomy, University of Sao Paulo Medical School, Ribeirão Preto, Brazil